ORIGINAL PAPER

Undecyl substitution in imidazole and its action on corrosion inhibition of copper in aerated acidic chloride media

Da-quan Zhang · Li-xin Gao · Guo-ding Zhou · Kang Yong Lee

Abstract Inhibition of copper corrosion by imidazole (IM) and 1-n-undecyl-imidazole (UDIM) in 0.5 M HCl was investigated by weight-loss measurements, potentiodynamic polarization curves and electrochemical impedance spectroscopy (EIS). 1-n-undecyl-imidazole showed the better inhibitive effect compared with IM. Potentiodynamic polarization results revealed that both IM and UDIM acted as anodic inhibitors, in particular UDIM suppressed anodic current densities significantly. Molecular structure parameters of IM and UDIM were obtained by using an MM2 forcefield program and AM1 quantum chemical calculation. It was found that UDIM has higher levels of HOMO and LUMO energy and a larger electron density in its imidazoly ring.

Keywords Copper · Acid corrosion · Weight loss · EIS · Polarization

1 Introduction

Benzotriazole (BTA) and its derivatives are effective inhibitors for copper and have been used in industry widely

D.-q. Zhang (✉) · L.-x. Gao · G.-d. Zhou
Department of Environmental Engineering, Shanghai University of Electric Power, Shanghai 200090, P.R. China
e-mail: zhdq@public9.sta.net.cn

K. Y. Lee
Stress Analysis and Failure Design Laboratory, School of Mechanical Engineering, Yonsei University, Seoul 120-749, Republic of Korea

for several decades [1–3]. However, a very important deficiency of these inhibitors is their toxicity and most of them cannot be biodegraded. This leads to the emission of industrial waste waters carrying a large amount of toxic material to waterways. Thus, their replacement by new environment-friendly inhibitors is desirable [4]. Stupnisek-Lisac et al. reported a series of imidazole (IM) derivatives as low-toxicity copper corrosion inhibitors [5]. Some Schiff bases were declared by Ma et al. to act as environmental-friendly copper inhibitors in aerated halide solution [6]. Rocca investigated linear sodium heptanoate as a non-toxic inhibitor for copper in 0.1 M Na_2SO_4 [7]. It was also shown that the substitution of alkyl-groups in the benzene ring exhibited higher inhibiting efficiency than that obtained for BTA [8]. Recently, development of organic compounds both containing hydrophilic and hydrophobic groups as corrosion inhibitors has gained attention. Controversy exists, however, on the actual role of the hydrophobic chains in relation to the improved inhibition. Amin used sodium oleate (an anionic surfactant inhibitor) to inhibit the acid corrosion of copper in 3% NaCl solutions [9]. He suggested that physical adsorption of the surfactant on the copper surface. The inhibitive action of the hydrophobic chains was attributed to the formation of a barrier layer on the copper surface, which retarded the diffusion of oxygen molecules from solution to copper substrate and increased the charge transfer resistance of anodic dissolution of copper. On the other hand, introducing substituents at different positions in azole compounds will influence the effective electron density and steric conformation of the molecule, from which is expected a concomitant influence on corrosion inhibition behavior [10–12]. It is still not clear which is more important on the inhibition property of hydrophobic chains, the physical barrier or its effect on the electron distribution

and steric conformation of the molecule inhibitor or the complex film.

Mechanistic information on corrosion and inhibition processes is very important for proper selection of inhibitors. A systematic approach is needed for characterization of the interaction between the organic inhibitor molecule and the metal or alloy. Such an approach should include inhibition studies utilizing molecular modeling. Bartley et al. employed molecular mechanics and molecular dynamics to simulate adsorption of alkyl esters of 5-carboxybenzotriazole on copper [13]. The objective of the present work was to investigate the action of the straight chain alkyl-group in IM to inhibit corrosion of copper in acidic chloride media. The abilities of IM and 1-n-undecylimidazole (UDIM) to inhibit copper corrosion in 0.5 M HCl solution were studied. Their inhibition efficiencies (IEs) were determined by coupon tests. Corrosion inhibition was investigated by means of potentiodynamic polarization curves and electrochemical impedance spectroscopy (EIS). The minimum energy conformation of these compounds was also obtained by the MM2 forcefield program. The relationship between molecular structure and inhibition efficiency was elucidated by AM1 (modified neglect of diatomic overlap, parametric method number) semi-empirical quantum chemical calculations. Molecular structure of IM and UDIM is shown in Fig. 1.

2 Experimental

2.1 Materials and apparatus

The coupons used for weight-loss measurements were circular copper discs (ϕ4.0 cm × 0.15 cm). The working electrode (WE) for electrochemistry measurements was prepared from a cylindrical copper rod (99.99%) sealed with epoxy resin so that only the circular cross section (0.4 cm^2) of the rod was exposed. IM and UDIM were AR grade and used as received. All other chemicals were AR grade and solutions were prepared using deionized water.

Electrochemical polarization curves and EIS measurements were performed in a three-electrode cell using a PARC M283 potentiostat (EG&G), PARC Model 1025
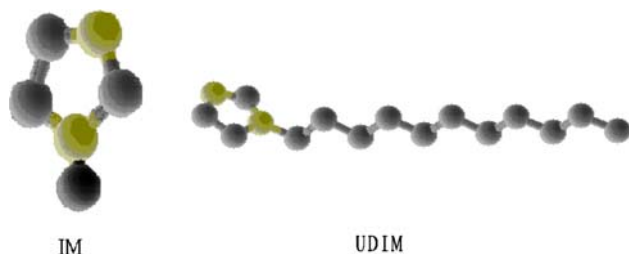

Fig. 1 Molecular structure of IM and UDIM

frequency response analyzer, and M352 and M398 software packages, respectively.

2.2 Weight-loss tests

Weight-loss measurements were carried out by suspending the coupons in 1000 mL vessel placed in a thermostat water bath (40 °C). The coupons were abraded with different grades of emery paper (#1, #4 and #6) and then washed and degreased with ethanol. They were then dried and rinsed with deionized water. These coupons with freshly prepared surfaces were then fully immersed in the quiescent 0.5 M HCl test solutions containing different inhibitors for 4 days. Studies were also done in solutions of different inhibitor concentration. All solutions were exposed to air. After the corrosion test, the corrosion products on the copper surface were removed by hard-rubber and the coupons were rinsed in deionized water and dried. The rinse removed loose segments of the film of the corroded samples. The mean corrosion rates (CRs) and IEs over the exposure period were calculated from the following equations:

$$CR = \frac{W_0 - W_1}{A \times T} \tag{1}$$

$$IE\% = \frac{CR_1 - CR_2}{CR_1} \times 100\% \tag{2}$$

where CR is in g m^{-2} h^{-1}; A is the specimen area (in m^2); W_0 is original weight of the specimen, and W_1 is specimen weight (in g) after the immersion period, T is the immersion period (in h), and CR_1 and CR_2 are the corrosion rates without and with inhibitor, respectively.

2.3 Electrochemical measurements

A three-electrode cell, employing a copper rod-working electrode (WE), platinum foil counter electrode, and saturated calomel electrode reference electrode (SCE) was used for measurements. The cell was open to air and the measurements were conducted at room temperature. All potential values are reported in mV (SCE). The WE was mechanically polished on emery paper (#1, #4 and #6), rinsed with deionized water, degreased with acetone and ethanol, and dried at room temperature. The degreased WE was inserted into the solution. After the corrosion potential (E$_{corr}$) became stable, it was then polarized from –800 mV to +900 mV at 1 mV s^{-1}. The EIS experiments were performed at open circuit potential over a frequency range 0.05 Hz to 100 kHz. The sinusoidal potential perturbation was 5 mV in amplitude. During the measurements, the solution was not stirred or deaerated.

3 Results and discussion

3.1 Weight-loss measurements

Corrosion rates of copper coupons were calculated by considering the total affected sample area and immersion times. The average CRs, expressed in g m^{-2} h^{-1}, are shown in Table 1.

As shown in Table 1, IM and UDIM inhibited the corrosion of copper in 0.5 M HCl solutions. IM showed better protection than UDIM below the 0.05 mM concentration level, while UDIM had superior inhibition compared with IM above this concentration. Concentration changes of IM below 0.5 mM lead to smaller changes in inhibition. UDIM showed increased inhibition with increasing concentration, and the best inhibition effect was observed when UDIM concentration reached above 0.1 mM. Increasing the concentration of UDIM increased IE up to a maximum value (72.4%) at 1.5 mM level, above which there was no evident increase. It is reported that maximum inhibition efficiency of surfactant is observed at concentrations around its critical micellar concentration (CMC). These results can be explained on the basis that, as the concentration of surfactant molecules approaches the CMC, micelles form in solution, and similar aggregate structures such as bilayers or multilayers form on surfaces [14]. In our previous study, the UV-Visible spectrum of UDIM in low concentration solution showed an absorption peak at approximately 209 nm. When the concentration of UDIM is above 0.5 mM, another absorption shoulder peak of 214 nm appeared. This is attributed to UDIM aggregate formation in the solution. The increase in UDIM

concentration enhances the intensity of the shoulder absorption peak [15]. These results show that the highest inhibition efficiency is obtained when the UDIM concentration reaches values close to its CMC.

3.2 Polarization curve measurements

3.2.1 Effect of inhibitor concentration

Figures 2 and 3 show the anodic and cathodic polarization curves of copper in 0.5 M HCl solutions with and without inhibitor. Anodic dissolution of copper in chloride media has been studied extensively [16, 17]. The mechanisms of anodic dissolution of copper in acidic chloride solutions are:

$$Cu + Cl^- \leftrightarrow CuCl_{ads} + e^- \tag{3}$$

$$CuCl_{ads} + Cl^- \leftrightarrow CuCl_2^- \tag{4}$$

The anodic curve for the copper electrode in a 0.5 M HCl solution exhibits two limiting current plateaus. This indicates a diffusion-limiting rate, probably due both to the transport of chloride (Cl$^-$) to the surface and the diffusion of (CuCl$_2^-$) in the solution. An anodic current peak A appeared at a potential of about –50 mV (SCE) and was related to CuCl film formation. The shapes of the curves in Fig. 2 show that the increase in IM concentration shifts the corrosion potential (E$_{corr}$) in the positive direction and reduces the anodic current density. Figure 2 shows that UDIM renders E$_{corr}$ more positive for the copper electrode in 0.5 M HCl solution. The active dissolution and passivity regions appeared for copper in the presence of UDIM. The active region showed apparent Tafel behavior with a slope close to 60 mV. It is evident that the introduction of

Table 1 Calculated corrosion rates (CR) and inhibition efficiency (IE) for weight-loss test in 0.5 M HCl solution (40 °C, 4 d)

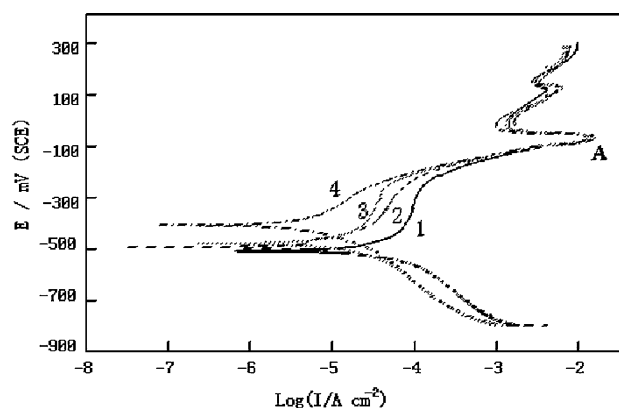| Inhibitors/mM	Weight-loss/g	CR/g m^{-2} h^{-1}	IE/%
Blank	0.83	3.44	–
0.01 mM IM	0.65	2.70	21.5
0.05 mM IM	0.64	2.65	23.0
0.1 mM IM	0.65	2.70	21.5
0.5 mM IM	0.65	2.70	21.5
1 mM IM	0.59	2.45	28.8
1.5 mM IM	0.56	2.32	32.6
2 mM IM	0.52	2.16	37.2
0.01 mM UDIM	0.74	3.06	11.0
0.05 mM UDIM	0.72	2.99	13.1
0.1 mM UDIM	0.31	1.29	62.5
0.5 mM UDIM	0.28	1.16	66.3
1 mM UDIM	0.25	1.03	70.1
1.5 mM UDIM	0.23	0.95	72.4
2 mM UDIM	0.23	0.87	72.4

Fig. 2 Polarization behavior of a copper electrode in 0.5 M HCl solution after 1 h immersion without (1) and with 0.05 mM of IM (2), 0.5 mM of IM (3) or 2 mM of IM (4)

n-undecyl to the IM ring leads to a large decrease in the anodic current density.

The cathodic corrosion reaction of copper in an aerated acidic chloride solution is

$$4H^+ + O_2 + 4e^- \rightarrow 2H_2O \qquad (5)$$

It is clear that the cathodic reaction shows a pseudo-Tafel region with and without inhibitor in 0.5 M HCl solution. The cathodic portion of the polarization curve is a composite and represents copper ion and oxygen reduction. The constancy of this cathodic slope in Fig. 2 indicates that the mechanism of the cathodic reaction is not changed by the addition of IM. As for UDIM, the cathodic polarization curve changes more in shape. The total copper corrosion reaction in acidic chloride solutions is [18]:

$$2Cu + 4H^+ + 4Cl^- + O_2 \rightarrow 2Cu^{2+} + 4Cl^- + 2H_2O \qquad (6)$$
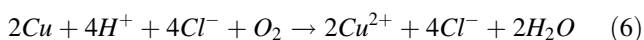
In general, both IM and UDIM acted as mixed inhibitors with the shift of E_{corr} to more positive values. The inhibition effect depended on concentration; the higher the concentration, the better the inhibition efficiency. UDIM showed the best inhibition effect for copper corrosion compared with IM at optimal concentration.

3.2.2 Effect of temperature

The influence of solution temperature on the corrosion behavior of copper in the presence of inhibitor was investigated. The anodic and cathodic polarization characteristics of copper in 0.5 M HCl solution are shown in Fig. 4 and 5.

Increase in solution temperature causes Ecorr to drift in the positive direction and enhances both the anodic and cathodic current densities. This may be attributed to the
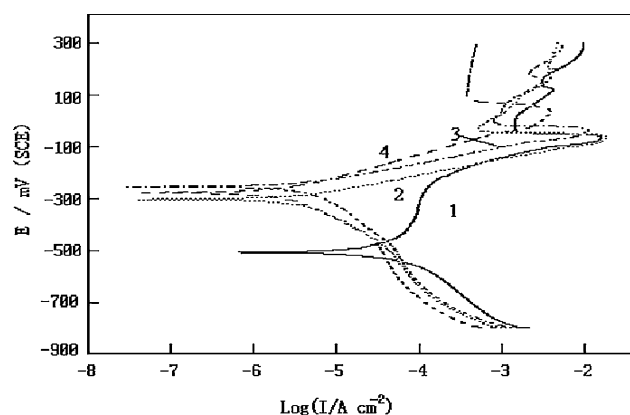

Fig. 4 Effect of temperature on the potentiodynamic curves of copper electrode in 0.5 M HCl containing 0.01 mM IM: (1–30 °C; 2–50 °C)
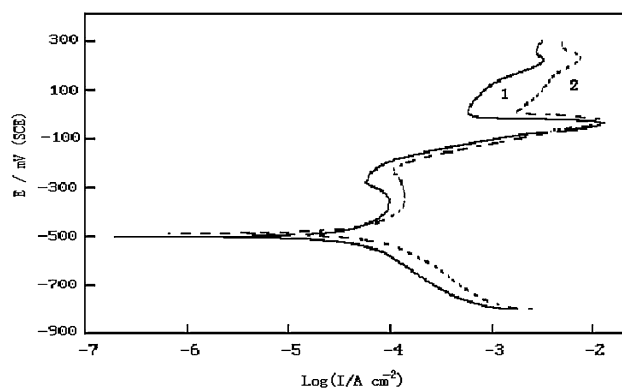
Fig. 5 Effect of temperature on the potentiodynamic curves of copper electrode in 0.5 M HCl containing 0.01 mM UDIM: (1–25 °C; 2–45 °C)

fact that an increase in temperature usually accelerates corrosive processes, giving rise to higher metal dissolution rates and a possible shift of the adsorption–desorption equilibrium towards desorption. This, as well as roughening of the metal surface as a result of enhanced corrosion, may also reduce the ability of the inhibitor to be adsorbed on the metal surface. The observed decrease in the strength of adsorption at higher temperatures suggests that physical adsorption may be the main type of adsorption of IM and UDIM [19].

3.2.3 Electrochemical impedance spectroscope (EIS)

Impedance measurements on the copper electrode were performed open to air at the open circuit potential. Figure 6 and 7 show the Nyquist plots for copper in 0.5 M HCl with IM or UDIM, respectively. A depressed semicircle with its center below the real axis was observed. This phenomenon is known as the dispersing effect [20]. As for 0.05 mM IM, the corrosion behavior of copper in this solution was

Fig. 3 Polarization behavior of a copper electrode in 0.5 M HCl solution after 1 h immersion without (1) and with 0.1 mM of UDIM (2), 0.5 mM of UDIM (3) or 2 mM of UDIM (4)
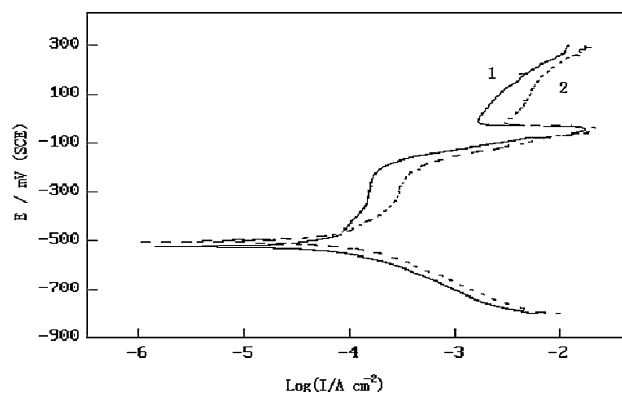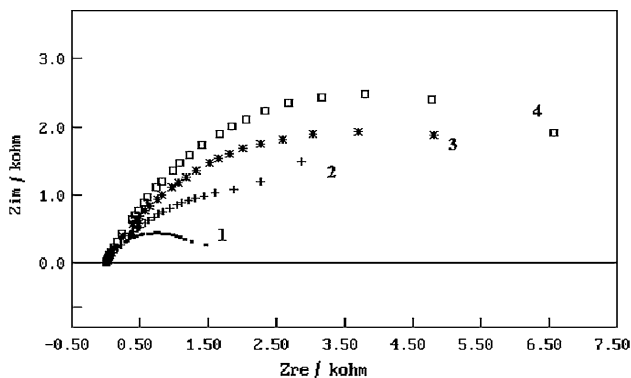
Fig. 6 Nyquist plots of a copper electrode in 0.5 M HCl solution without (1) and with 0.05 mM IM (2), 0.5 mM IM (3), and 1.5 mM IM (4)
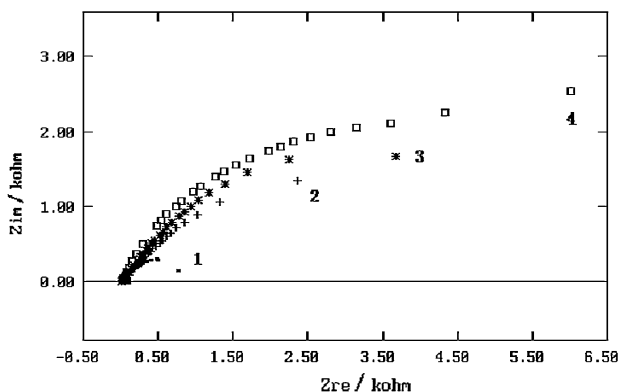

Fig. 7 Nyquist plots of a copper electrode in 0.5 M HCl solution without (1) and with 0.1 mM UDIM (2), 1 mM UDIM (3), and 2 mM UDIM (4)

influenced, to some extent, by mass transport since a Warburg impedance plot was observed in the low frequency region, while a similar Warburg impedance plot was obtained for 2 mM UDIM. The Nyquist plots do not show a straight-line portion at low frequencies because of the limited low frequency range.

The equivalent circuit model employed for this system is shown in Fig. 8. It contains of solution resistance R_s in series connection with two time constants. The first time constant, $R_t C_{dl}$, in the high frequency region is proposed to be a result of the fast charge transfer process of copper dissolution, R_t being the charge transfer resistance and C_{dl} the double layer capacitance. Since electrochemical systems show various types of inhomogeneity [21], C_{dl} can be better substituted by a constant phase element (CPE). The CPE element was introduced formally only for fitting impedance data. The second time constant in the low impedance region results from mass transport through the oxide film, C is the capacitance of the surface film, and R_2 is the surface layer resistance.

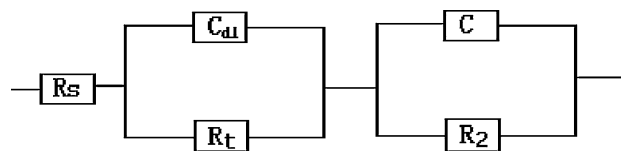The total impedance Z of the electrochemical system is given by

Fig. 8 Equivalent circuit model for the corrosion of copper

Table 2 Electrochemical parameters for corrosion of copper in 0.5 M HCl after 40 minutes immersion

Inhibitor	R_t/kΩ cm^2	Q/μF cm^{-2}	n	R_2/kΩ cm^2	C/μF cm^{-2}
Blank	1.33	195	0.741	0.130	124
0.05 mM IM	3.18	168	0.718	0.001	155
0.5 mM IM	5.79	117	0.725	0.113	102
1.5 mM IM	7.55	94	0.750	0.395	147
0.1 mM UDIM	5.53	474	0.582	0.117	110
1 mM UDIM	7.31	278	0.610	0.587	78
2 mM UDIM	8.24	157	0.692	0.889	73

$$Z = R_{sol} + \frac{R_t}{1 + R_t Q(j\varpi)^n} + \frac{R_2}{1 + R_2 j\varpi C} \qquad (7)$$

The quantitative analysis of the experimental impedance data was conducting by a computer program EQUIVCRT based on a nonlinear least squares minimization method developed by Boukamp [22]. The electrochemical impedance parameters derived from these figures are given in Table 2.

The R_t value was used to compare the effect of the inhibitor. The more densely packed the inhibitor surface film, the larger the diameter of the semicircle, which results in higher R_t and lower C_{dl} values. It is clear that the presence of the inhibitor increases the impedance of the copper electrode and the charge transfer resistance (R_t) values increase with increasing inhibitor concentration. R_t in the presence of UDIM is greater than with IM. The decrease in the C_{dl} values with increasing IM concentration is due to inhibitor adsorption on the copper surface. C_{dl} in the presence of UDIM is greater than that in blank 0.5 M HCl solution. This can be explained by the different adsorption behavior of UDIM compared with IM. These results suggest that UDIM has the better protection effect. The effect of molecular structure on corrosion inhibition was the same as that determined using the weight-loss method and electrochemical measurements.

3.3 AM1 quantum chemical calculations

Quantum chemical calculations were carried out at the Restricted Hartree–Fock level (RHF) using AM1 semi-

Table 3 Quantum chemical parameters calculated by AM1 semi-emperical method

Inhibitor	E_{HOMO}/eV	E_{LUMO}/eV	Net atomic charges					
			C1	C2	N3	C4	N5	Ring$_{total}$
IM	−11.59974	−6.18405	0.0203	0.1696	−0.4035	0.2504	−0.3143	−0.2775
UDIM	−8.12834	−4.02918	−0.0038	0.0030	−0.2657	0.1015	−0.3659	−0.5309

empirical SCF-MO methods in the MOPAC 7.0 program. RHF means the restricted Hartree–Fock Hamiltonian is to be used [23]. Table 3 shows the energy (in eV) of the highest occupied molecular orbital (HOMO) and the lowest unoccupied molecular orbital (LUMO) for inhibitors and the electron density for atoms in the IM ring. It has been reported that the higher the HOMO energy (E_{HOMO}) level of the inhibitor, the greater is the ease of offering electrons to the unoccupied d orbital of metallic copper and the greater the inhibition effciency [24]. The present results show that UDIM has a better protective effect for copper corrosion and has higher E_{HOMO} and E_{LUMO} values compared with IM.

It has also been reported that inhibitors can form coordination bonds between the unshared electron pair of the N atom and the unoccupied d electronic orbital of the metal [25]. The larger the negative charge of the N atom, the better is the action as an electronic donor. Previous studies showed that the adsorption of 1,2,4-triazole and IM on copper may be in a manner in which the plane of the inhibitor molecule is parallel to the metal surface [26]. Thus, the better inhibition efficiency of UDIM for copper corrosion in HCl solution can also be attributed to its larger ring electron densities. It has been reported previously that an alkyl chain present in the inhibitor molecular can form a hydrophobic barrier retarding the metal corrosion in aggressive environments [27]. Our present study shows that the introduction of an undecyl to a IM ring can vary the disturbances and orbital energy configuration of electrons, thus enhancing the inhibitory effects on copper corrosion in 0.5 M HCl solutions.

4 Conclusion

The inhibition effects of IM and its undecyl derivative on copper corrosion were investigated in aerated HCl solution. Substitution in the IM ring results in an increase in inhibiting efficiency in relation to IM at an optimal concentration. It seems that the introduction of an undecyl to an IM ring improves its inhibitory effect by varying the disturbances and orbital energy configuration of electrons.

References

1. Notoya T, Poling GW (1976) Corrosion 32:216
2. Mansfeld F, Smith T, Parry P (1971) Corrosion 27:289
3. Chadwick D, Hashemi T (1978) Corros Sci 20:1881
4. Stupnisek-Lisac E, Loncaric Bozic A, Cafuk I (1998) Corrosion 54:713
5. Gasparac R, Stupnisek-Lisac E (1999) Corrosion 55:1031
6. Ma H, Chen S, Niu L, Zhao S, Li S, Li D (2002) J Appl Electrochem 32:65
7. Rocca E, Bertrand G, Rapin C, Labrune JC (2001) J Electroanal Chem 503:133
8. Huynh N, Bottle SE, Notoya T, Schweinsberg DP (2000) Corros Sci 42:259
9. Amin MA (2006) J Appl Electrochem 36:215
10. Otieno-Alego V, Hope GA, Notoya T, Schweinsberg DP (1996) Corros Sci 38:213
11. Schweinsberg DP, Bottle SE, Otieno-Alego V (1997) J Appl Electrochem 27:161
12. Otmacic H, Telegidi J, Papp K, Stupnisek-lisac E (2004) J Appl Electrochem 34:545
13. Bartley J, Huynh N, Bottle SE, Flitt H, Notoya T, Schweinsberg DP (2003) Corros Sci 45:81
14. Abd El-Rehim SS, Hassan HH, Amin MA (2002) Mater Chem Phys 78:337
15. Zhang DQ, Gao LX, Zhou GD (2002) J Chin Soc Corros Prot 22:237
16. Brusic V, Frish MA, Eldridge BN, Novak FP, Koufman FB, Rush BM, Frankel GS (1991) J Electrochem Soc 138:2253
17. Tromans D, Sun R, (1991) J Electrochem Soc 138:3235
18. Zhang DQ, Gao LX, Zhou GD (2004) Corros Sci 46:3031
19. Oguzie EE, Onuoha GN, Onuchukwu AI (2004) Mater Chem Phys 89:305
20. Li SL, Ma HY, Lei SB, Yu R, Chen SH, Liu DX (1998) Corrosion 54:947
21. Benedetti AV, Sumodjo PTA, Nobe K, Cabot PL, Proud WG (1995) Electrochim Acta 40:2657
22. Boukamp BA (1980) Solid State Ionics 20:31
23. Moretti G, Guidi F, Grion G (2004) Corros Sci 46:387
24. Ogretir C, Mihci B, Bereket G (1999) J Mol Struct 488:223
25. Wang D, Li S, Ying Y, Wang M (1999) Corros Sci 41:1991
26. Thierry D, Leygraf C (1986) J Electrochem Soc 133:2237
27. Ma H, Chen S, Yin B, Zhao S, Liu X (2003) Corros Sci 45:867